Enhanced Performance of Organic Photodetector Through Metal Doping and Inkjet Printing for Sensor-in-Pixel Displays

*Gun Woong Kim†, Jaebum Jeong† and Jun Young Kim†,**

† Department of Semiconductor Engineering,

Gyeongsang National University, Jinju-City, Gyeongsangnam-do, Republic of Korea

Abstract

We developed an inverted OPD by doping the hole-blocking layer with metals, reducing leakage current and enhancing detection performance under reverse bias. IGZO-doped devices exhibited the best leakage current suppression and specific detectivity. Inkjet printing was applied to achieve precise pixelation of the OPD layers, highlighting its potential for large-area, solution-processed Sensor-in-Pixel displays. This work demonstrates the feasibility of OPD fabrication for wearable and security applications.

Author Keywords

Organic photodetector (OPD); Leakage current (dark current); blocking layer; InGaZnO (IGZO); Sensor-in-pixel (SIP); Inkjet printing process.

1. Introduction

Organic photodetectors (OPDs) have seen rapid advancements and are increasingly integrated into various devices [1]. In wearable technologies such as smartwatches, OPDs function as vital health monitoring sensors, measuring parameters like heart rate, oxygen saturation, and blood glucose levels. Additionally, they play a critical role in security applications, such as fingerprint recognition, enabling user authentication [2-5]. The functionality of these sensors relies on the ability of organic materials to absorb light within specific wavelength ranges. To achieve this, a light source, such as a light-emitting diode (LED), with specific wavelengths is essential. While sensors and LEDs are currently designed as separate components, the growing demand for device miniaturization and enhanced integration necessitates a shift toward pixel-level integration of these elements like Sensor-in-pixel (SIP) displays [6]. Most research has primarily focused on physical vapor deposition (PVD) based fabrication, emphasizing the need for solution-processable methods for large-area production [7].

Despite the advantages offered by organic materials, such as selective light absorption through chemical composition control, flexibility, and cost-efficiency, several challenges remain in the application of organic photodetectors (OPDs) to SIP displays when compared to silicon-based sensors. These challenges include leakage current, response speed, and stability. Specifically, leakage current arises from the reverse bias operation characteristics of typical photodetectors, where no current should flow in the absence of light. However, in the case of organic materials, a higher leakage current is observed compared to silicon. This is attributed to structural defects in devices containing organic materials, where electrons and holes are collected by electrodes under an electric field. To address this issue, methods such as designing the band energy of the organic material or incorporating a blocking layer that serves as a charge barrier are employed [8].

To enhance the leakage current blocking characteristics, zinc oxide (ZnO) was doped with indium, gallium, and aluminum, used as a hole-blocking layer, and an inverted structure organic photodetector (OPD) device was fabricated. The performance of each metal-doped device in blocking leakage current was evaluated, revealing a reduction in reverse bias leakage current and an improvement in the performance indicator, specific detectivity (D*). Notably, the device InGaZnO (IGZO) doped with indium and gallium exhibited the highest detection characteristics. Furthermore, pixelization of the blocking and photosensitive layers using inkjet printing suggests the potential application of solution-processed OPD devices in Sensor-in-Pixel (SIP) display technology.

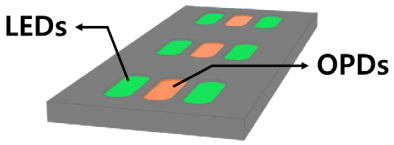

Figure 1. Schematic Diagram of a SIP Display Structure

2. Results and Discussion

The fundamental structure of organic photodetectors (OPDs) resembles that of solar cells, with a photoactive layer positioned between two electrodes. This layer absorbs specific wavelengths of light and facilitates the dissociation of excitons into electrons and holes. The separated charges are transported through charge transport layers to their respective electrodes, where they are collected and converted into electrical signals. To enhance charge separation efficiency, the photoactive layer adopts a bulk heterojunction (BHJ) structure. This structure involves blending donor and acceptor materials at a specific ratio, which significantly increases the interfacial area compared to bilayer structures. Additionally, it allows for controlled crystalline, further improving charge separation efficiency. In this study, the active layer was composed of PBDB-T as the donor and Y6-Cl as the non-fullerene acceptor, blended at a 1:1.2 ratio. The anode consisted of silver (Ag), while molybdenum trioxide (MoO_3) served as the hole transport layer (HTL). To suppress leakage current, a blocking layer made of ZnO doped with various metals was inserted between the active layer and the indium tin oxide (ITO) cathode. The fabrication process involved spin coating for the active and blocking layers, while the HTL and Ag were deposited via thermal evaporation.

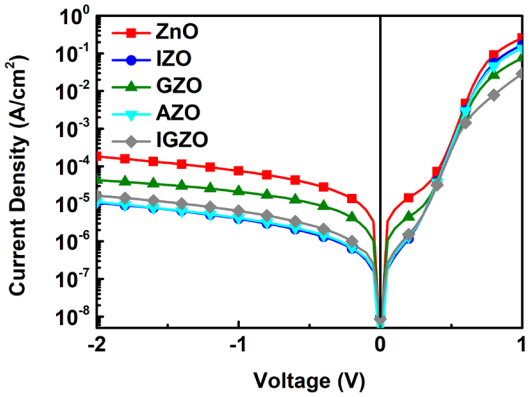

Figure 2. J-V Characteristics of OPDs in Dark Conditions for Different Metal Doping Combinations

ISSN 0097-996X/25/5603-2099-$1.00 © 2025

$$D^* = \frac{R}{\sqrt{2qJ_{dark}}}[Jones] \quad (1)$$

The specific detectivity (D*) is a key figure of merit for evaluating the performance of OPDs, as it represents their ability to detect weak optical signals with high sensitivity [9]. The calculation of D* relies on two fundamental parameters: the dark current density (J_d) and the responsivity (R). J_d represents the current flowing through the device under dark conditions, while R is defined as the photocurrent generated per unit of incident light power at a specific wavelength. Additionally, q is the elementary charge, 1.6 × 10^{-19} C.

Figure 2 presents the current density-voltage (J-V) characteristics of OPD devices under dark conditions, fabricated using blocking layers doped with various metal combinations (indium, gallium, and aluminum). The measurements were performed over a voltage range from -2V to 1V, including the reverse bias operating voltage, with current density displayed on a logarithmic scale. It was observed that the current density decreases progressively with doping combinations in the following order: ZnO, GZO, IGZO, AZO, and IZO. Notably, the devices with IGZO, AZO, and IZO exhibit similar current densities at -2V, with values of 1.65 × 10^{-5} A/cm², 1.1 × 10^{-5} A/cm², and 1.06 × 10^{-5} A/cm², respectively. These values are significantly lower than the current density of the undoped ZnO device, which shows 1.83 × 10^{-4} A/cm², indicating a reduction of up to 17 times. This substantial decrease highlights the effectiveness of doping in enhancing the leakage current suppression properties of the devices.

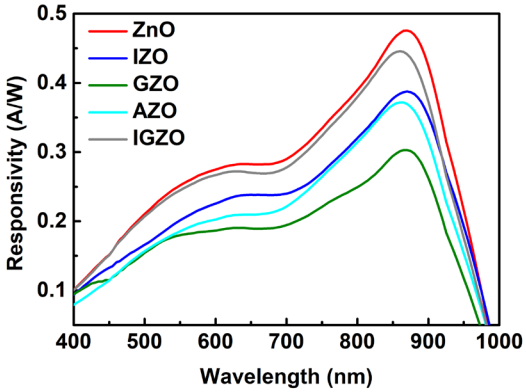

Figure 3. Responsivity of OPDs at -2 V Bias for Different Metal Doping Combinations

The responsivity spectra of OPD devices under different metal doping conditions are shown, highlighting their ability to convert incident light into electrical current at specific wavelengths (Figure 3). The X-axis represents the wavelength range, spanning from 400 nm to 1000 nm, which covers both visible and near-infrared regions. The Y-axis shows the responsivity values expressed in amperes per watt (A/W), indicating the efficiency of the donor-acceptor materials in the active layer across this spectral range. The devices exhibit a distinct peak at 865 nm, with ZnO achieving the highest responsivity of 0.47522 A/W across the entire spectrum. The responsivity decreases in the order of IGZO, IZO, AZO, and GZO. The reduction in responsivity for doped devices compared to undoped ZnO is likely due to defect formation caused by doping. These defects can degrade charge carrier mobility and absorption properties, resulting in increased recombination and reduced absorption efficiency. Additionally, ZnO is an excellent material, as demonstrated in many studies, and its high sensitivity can be attributed to its optimized composition. Among the doped devices, IGZO achieves a responsivity of 0.44489 A/W, slightly lower than ZnO, followed by IZO (0.38669 A/W), AZO (0.3717 A/W), and GZO (0.3031 A/W). These findings indicate that while ZnO exhibits the best responsivity, IGZO, with its superior leakage current characteristics, also shows great potential as a viable material.

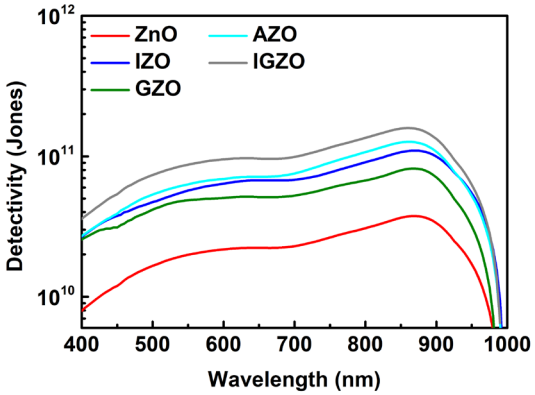

Figure 4. Detectivity of OPDs at -2 V Bias for Different Metal Doping Combinations

The detection characteristics of OPD devices with various metal doping combinations were calculated based on the leakage current characteristics and the light sensitivity spectra, and the results were plotted in Figure 4. The X-axis represents the wavelength spectrum, and the Y-axis shows the calculated D* values on a logarithmic scale, expressed in Jones. The device with IGZO exhibited the highest detection performance, with a D* value of 1.59 × 10^{11} Jones. The Jones values decrease in the following order: AZO, IZO, GZO, and ZnO. Overall, the doped devices show at least a two-fold increase in D* compared to ZnO without doping. This improvement in detection performance can be attributed to the enhanced leakage current characteristics resulting from doping, with IGZO showing the most favorable leakage current properties and good light sensitivity, thereby achieving the highest D*. On the other hand, ZnO, with a D* value of 3.75 × 10^{10} Jones, exhibits the best light sensitivity characteristics but has very poor leakage current properties, leading to the lowest D* value. These results indicate that doping not only improves leakage current characteristics but also plays a crucial role in enhancing detection performance. This is likely due to an increase in the bandgap energy caused by metal doping, which results in a decrease in the HOMO level. As a result, the probability of hole injection from the electrode to the blocking layer in a reverse bias decrease, thereby reducing the leakage current [10-12].

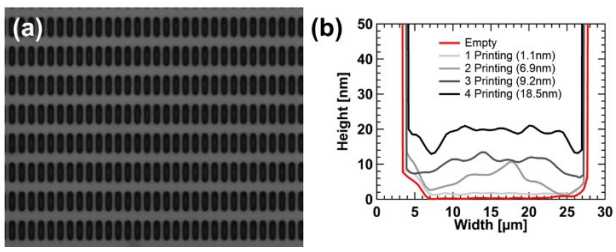

Figure 5. Inkjet Printing Based ZnO and Active Layers on

200 PPI Substrate: (a) Planar Image of ZnO Layer, (b) Cross-section Graph of BHJ Active Layer as a Function of Printing Count

Figure 5 illustrates the results of inkjet printing processes applied to ZnO and the active layer, previously formed by spin coating. The micro-patterning was conducted on a 200 PPI substrate with sub-pixel dimensions of 24 × 84 μm and a depth of 1.5 μm. (a) shows the image of the printed ZnO layer captured using the imaging tool of the printing equipment, revealing precise printing without any overlap into adjacent pixels. Meanwhile, (b) presents the cross-sectional thickness of the active layer measured after varying the number of printing cycles, obtained from a 3D profiler. The cross-sectional data were converted into a graph, where the red line represents an empty pixel. With an increasing number of printing cycles, the thickness of the active layer gradually increases. However, significant surface non-uniformity was observed, which could lead to unfavorable leakage current due to localized regions facilitating easier current flow. To address this issue, analyzing the properties of the ink is crucial [13]. Key characteristics include the ink's viscosity, which determines its flow behavior during deposition; boiling point, which influences drying dynamics; and surface tension, which governs interactions between ink droplets. Additionally, drying conditions must be carefully controlled, as the ink properties vary significantly depending on whether a single solvent or a solvent mixture is used [14-15]. While prior approaches primarily relied on natural drying or controlled temperature environments, recent studies have adopted vacuum conditions to enhance surface uniformity [16]. We plan to achieve surface uniformity using these methods, followed by pixelization of the OPD. This approach is expected to be actively utilized in the development of SIP display technologies for smartphones and smartwatches.

3. Conclusion

We investigated the impact of metal doping combinations to improve the D* of OPDs. Devices incorporating IGZO showed a 17 times reduction in leakage current compared to ZnO, leading to significantly enhanced D*. By applying the inkjet printing process, precise pixelation was achieved on a 200 PPI substrate, demonstrating the potential of solution-processed OPD devices for SIP display technology. Also, we plan to address the surface uniformity issue by controlling drying conditions to enhance the process of fabricating OPD devices based on inkjet printing.

4. Acknowledgements

This work was supported by the National Research Foundation of Korea (NRF) grant funded by the Korea government (MSIT) (No. RS-2023-00222166) and the GNU-Samsung Display Center.

5. References

1. Xia Y, et al. High-Speed Flexible Near-Infrared Organic Photodetectors for Self-Powered Optical Integrated Sensing and Communications. *Adv. Funct. Mater*. 2024: 2412813.
2. Luo G, et al. Boosting the Performance of Organic Photodetectors with a Solution-Processed Integration Circuit toward Ubiquitous Health Monitoring. *Adv. Mater*. 2023;35(36):2301020.
3. Tang L, Chang SJ, Chen C-J, Liu J-T. Non-invasive blood glucose monitoring technology: a review. *Sensors*. 2020;20(23):6925.
4. Tordera D, et al. A high-resolution thin-film fingerprint sensor using a printed organic photodetector. *Adv. Mater. Technol*. 2019;4(11):1900651.
5. Kim C, et al. Sensor organic light-emitting diode display, combining fingerprint and biomarker capturing. *Communications Engineering*. 2024;3(1):92.
6. Min WK, et al. Strain-Sensor-In-Pixel Technology for Resolution-Sustainable Stretchable Displays. *ACS nano*. 2024;18(27):17735-48.
7. Wang Y, et al. Semitransparent Near-Infrared Organic Photodetectors: Flexible, Large-Area, and Physical-Vapor-Deposited for Versatile Advanced Optical Applications. *Adv. Funct. Mater*. 2024:2313689.
8. Yang D, Ma D. Development of organic semiconductor photodetectors: from mechanism to applications. *Adv. Optical Mater*. 2019;7(1):1800522.
9. Li Y, Chen H, Zhang J. Carrier blocking layer materials and application in organic photodetectors. *Nanomaterials*. 2021;11(6):1404.
10. Yang W, et al. Mitigating dark current for high-performance near-infrared organic photodiodes via charge blocking and defect passivation. *ACS Appl. Mater. Interfaces*. 2021;13(14):16766-74.
11. Shan T, Hou X, Yin X, Guo X. Organic photodiodes: device engineering and applications. *Frontiers of Optoelectronics*. 2022;15(1):49.
12. Joshi K, et al. Band gap widening and narrowing in Cu-doped ZnO thin films. *Journal of Alloys and Compounds*. 2016;680:252-8.
13. Ren M, et al. Inkjet printing technology for OPV applications. *Journal of Imaging Science and Technology*. 2012;56(4):40504-1-5.
14. Singh M, Haverinen HM, Dhagat P, Jabbour GE. Inkjet printing—process and its applications. *Adv. Mater*. 2010;22(6):673-85.
15. Tao R, et al. Capillary force induced air film for self-aligned short channel: Pushing the limits of inkjet printing. *Soft Matter*. 2018;14(46):9402-10.
16. Han YJ, et al. Sequential improvement from cosolvents ink formulation to vacuum annealing for ink-jet printed quantum-dot light-emitting diodes. *Materials*. 2020;13(21):4754.